Sizing Optimization with Thermal and Electrical Matching of a Thermogenerator placed on the Human Body

Marianne LOSSEC, Bernard MULTON and Hamid BEN AHMED
SATIE, ENS Cachan Antenne de Bretagne, CNRS, UEB
Tel: +33(0)299059322 – e-mail: marianne.lossec@bretagne.ens-cachan.fr

Topics: Energy harvesting

1. Introduction

As part of the study of a multisource generator harvesting resources of the human environment [1] (heat, light, movement), we studied the potential of thermoelectric generation from human body heat. The main objective is to maximize the thermoelectric productivity with a view to charging an accumulator which itself supplies a consumer electronic device such as a communicating sensor.

To this end, thermogeneration [2,3] consists in placing one side of a thermoelectric module into contact with the skin of human body and the other in direct contact with ambient air, possibly via a heatsink. The difference in temperatures between the two sides is then used to directly convert heat into electricity. However, the output voltage of the thermoelectric generator (TEG) is relatively low, this being mainly due to bad thermal coupling of the generator with its environment [4]. In addition the number of thermocouples in series is limited by the integrating constraints and the available area. For all these reasons, a matching converter is necessary to increase the voltage in order to connect the generator to a storage element where the voltage is typically between 1 and 4 V depending on the technology used. Fig. 1 shows a diagram of the system studied.
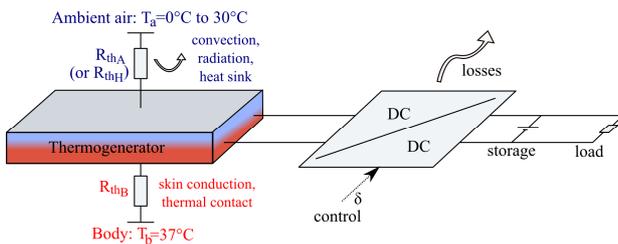

Figure 1: Thermoelectric generation system from the human body

The sizing of such a device should be done with a system-level approach where the thermal coupling with the environment, and the electrical coupling with the DC-DC converter (including losses) are taken into account. The advantage of such an approach is presented in this article. The dual thermal and electrical matching that maximize energy harvesting will also be studied.

2. Study of thermoelectric generator (TEG)
2.1. Thermal and electrical models of TEG

In the particular context of harvesting energy from the human body, thermal and electrical models of the TEG are shown in Fig. 2. These benchmark models have been validated [4] from experiments performed with the thermoelectric module TM-450-0.8-3.0 produced by Ferrotec company. This module, made of bismuth telluride, has 450 thermocouples for a surface area of about 30cm^2 and a height of 1.5mm.
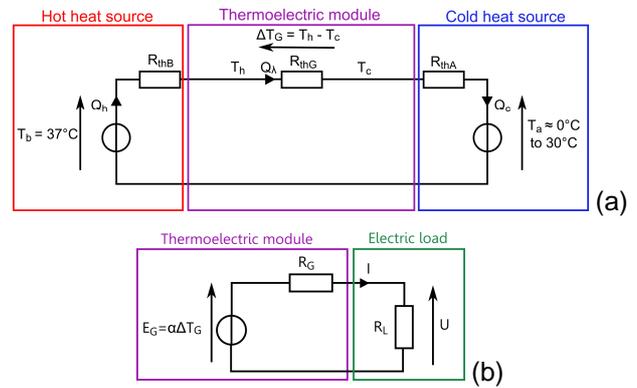

Figure 2: Simplified thermal (a) and electrical (b) models of the TEG

The distinctive feature of such a system in human environment is the very low resources available and the poor thermal coupling with the environment resulting in a low effective difference in temperatures between hot and cold heat sources. According to the powers recoverable, the human body and the environment can be considered as infinite sources of temperature, unaffected by the presence of the TEG. Couplings of the hot and the cold sides with temperatures T_b and T_a are represented by two thermal resistances R_{thB} and R_{thA}. R_{thB} is the thermal resistance between the hot heat source (here the human body) and the hot side of the module. It corresponds to the thermal conduction resistance of the skin and of the thermal contact between the surface of the skin and the hot side of the module. R_{thA} is the thermal resistance between the cold side of the module and the surrounding air. It corresponds to radiation and natural convection of the cold side with ambient air. A pin fin heat sink can also be added (increasing the size) to improve heat transfer. In this case we denote R_{thH} the thermal resistance of the heat sink. In addition to these two resistances, the thermal resistance R_{thG} represents heat conduction through all N_{th} thermocouples, which are

thermally connected in parallel, and constitute the TEG. From a purely electrical standpoint, the N_{th} thermocouples are electrically connected in series and therefore have a total electrical resistance denoted R_G. Thus, the TEG behaves like an electromotive force (emf) E_G (proportional to the difference in temperatures at its thermal faces ΔT_G and to Seebeck coefficient α) associated to an internal resistance R_G.
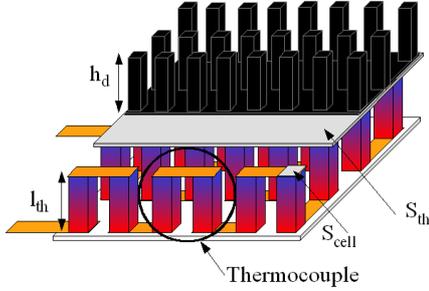

Figure 3: Definitions of the TEG notations

Considering the notations defined in Fig. 3, and denoted ρ and λ respectively the electrical resistivity and the thermal conductivity of a thermocouple (average of the two materials), h_A and h_B the heat transfer coefficients on both sides of the TEG, and k_f the filling factor of the thermocouples in the TEG, we can express the thermal and electrical resistances previously defined by:

$$R_{thB} = \frac{1}{h_B S_{th}}; \quad R_{thG} = \frac{l_{th}}{\lambda k_f S_{th}}$$

$$R_{thA} = \frac{1}{h_A S_{th}}; \quad R_G = N_{th}^2 \rho \frac{4 l_{th}}{k_f S_{th}} \quad (1)$$

As already pointed out, adding a heat sink enhances the thermal coupling between the cold side of TEG and ambient air [5]. Its thermal resistance R_{thH} depends on its captation surface area S_{th} and on its height h_d. We studied the heat sink datasheets produced by Aavid company in order to establish a thermal model. Fig. 4 shows, for different fin height h_d, the variation of R_{thH} according to the surface area S_{th} (the points correspond to the values found in the datasheet and the solid lines to the model set). Note that we extrapolated this model because the maximum surface area of the heat sinks produced by Aavid was only 16cm².
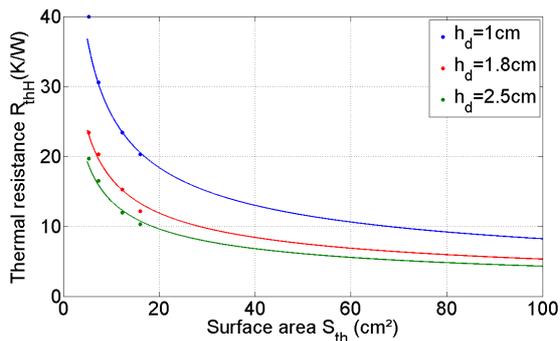

Figure 4: Thermal model of the heat sink

The study of Aavid heatsinks led us to the following model, the coefficients k_{H1} and k_{H2} being constant:

$$R_{thH} = \left(\frac{k_{H1}}{h_d} + k_{H2} \right) \frac{1}{\sqrt{S_{th}}} \quad (2)$$

Note that the fact that the thermal resistance R_{thH} is inversely proportional to $\sqrt{S_{th}}$ assumes that convection effects are solely due to the fins present on the perimeter of the heat sink.

The thermal and electrical models presented above enable us to express the emf E_G of the TEG. We denote α_0 the Seebeck coefficient of a thermocouple and ΔT_0 the difference in temperatures between the hot source T_b and cold source T_a.

$$E_G = N_{th} \alpha_0 \Delta T_0 \frac{l_{th}}{l_{th} + k_{env}} \quad (3)$$

The coefficient k_{env} depends on the presence or not of the heat sink and is expressed as follows:

$$k_{env} = \lambda k_f \left(\frac{1}{h_B} + \frac{1}{h_A} \right) without\ heat\ sink$$

$$k_{env} = \lambda k_f \left(\frac{1}{h_B} + \sqrt{S_{th}} \left(\frac{k_{H1}}{h_d} + k_{H2} \right) \right) with\ heat\ sink \quad (4)$$

Taking into account the values defined in Table 1, Fig. 5 shows the emf E_G, with and without heat sink, according to the leg length l_{th}.

Table 1: Parameter values associated with TEG and its environment

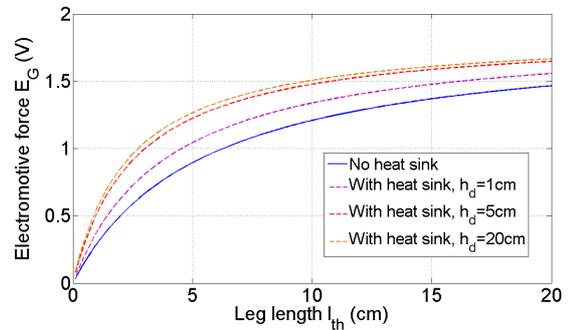| N_{th}	450	S_{th}	30 cm²
α_0	267 µV.K^{-1}	T_b	37.5°C
λ	0.77 W.m^{-1}.K^{-1}	T_a	22°C
ρ	20 µΩ.m	h_B	25 W.m^{-2}.K^{-1}
k_f	0.6	h_A	13 W.m^{-2}.K^{-1}

Figure 5: Evolution of the emf E_G according to the leg length l_{th}

Whatever the electrical load R_L connected to the TEG, the electrical power P_e recoverable is expressed as follows:

$$P_e = \frac{k_c k_f \alpha_0^2 \Delta T_0^2}{4\rho} \frac{S_{th} l_{th}}{\left(l_{th} + k_{env}\right)^2} \qquad (5)$$

The coefficient k_c depends on the electrical operating point of the TEG. For an electrical impedance matching, it is equal to ¼. In this case, the electrical power recoverable is maximum, we denote it P_{em}. Fig. 6 shows the evolution of this power, with and without heat sink, according to the leg length l_{th}. This shape is known and shows an optimum value for the leg length, but this length is generally not technologically feasible (too high). One way to achieve substantially the same improvement can be to stack the modules [3,4] as we are highlighting below.
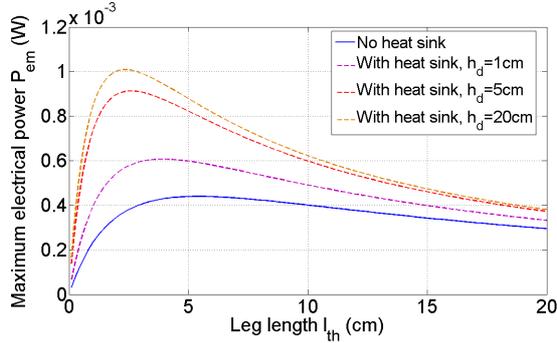

Figure 6: Evolution of the power P_{em} according to the leg length l_{th}

2.2. Thermal impedance matching

A fundamental problem of harvesting energy from the human body is linked to poor thermal matching of the TEG with its environment. In other words, the thermal resistance R_{thG} is generally very low compared to those related to environment R_{thB} and R_{thA} (or R_{thH} with a heat sink). We denote R_{thE} the sum of thermal resistances related to the environment, i.e. $R_{thB} + R_{thA}$ without a heat sink, and $R_{thB} + R_{thH}$ with a heatsink. Since the internal thermal and electrical resistances of the TEG, respectively denoted R_{thG} and R_G, are proportional to the leg length l_{th}, its increase improves the thermal coupling and thus increases ΔT_G but also enhances the internal resistance R_G and therefore a priori decreases the maximum electrical power harvested. Considering equation (5), we can show that the electrical power is maximum for an optimum value of l_{th} [6], which differs according to the heat sink presence, and which is expressed as follows:

$$l_{th\_opt} = \lambda k_f \left(\frac{1}{h_B} + \frac{1}{h_A} \right) without\ heat\ sink$$

$$\qquad (6)$$

$$l_{th\_opt} = \lambda k_f \left(\frac{1}{h_B} + \sqrt{S_{th}} \left(\frac{k_{H1}}{h_d} + k_{H2} \right) \right) with\ heat\ sink$$

This maximum power is obtained when the internal thermal resistance of the TEG R_{thG} is equal to the sum of thermal resistances of its environment,

i.e. to R_{thE}. The difference in temperatures across the TEG ΔT_G is thus equal to half the difference in temperatures between the body and the ambient [7], which corresponds to a thermal impedance matching.

A solution to improve energy harvesting, given a surface area of the TEG, is to stack identical thermoelectric modules and to connect them electrically in series [3,4]. Stacking thermoelectric modules finally amounts to increasing the leg length l_{th} of the TEG. Thus increasing the leg length or stacking thermoelectric modules improves the thermal coupling for a given surface area and thus increase the emf and the electrical power of the TEG. This result proves to be a considerable advantage when connecting the TEG to a DC-DC converter. We will understand why below in the article.

3. Study of the whole system with DC-DC converter

3.1. Electrical model of the converter

The DC-DC converter that serves as our benchmark is the LTC3537 from Linear Technology [8]. This is a very low voltage synchronous boost converter with two dual-gate MOS transistors, one used for the transistor function and the other to replace the diode, which significantly reduces conduction losses. The dual-gate MOS technology extends the range of the maximum converter efficiency thanks to a change in operating mode into low power which shows itself by a switching between the two gates. The difference between the two gates is the controlled semiconductor area: we denote k_G, higher than 1, the ratio between the two electrode areas. The gate charge Q_G is proportional to the area while the channel resistance r_{dson} is inversely proportional. Thus, the solution adopted by the LTC3537 converter is to drive the gate with a small area at low powers, where the losses related to the control gate become predominant, and to drive the gate with a large area at high powers. This concept is described in [9]. We denote k_M a coefficient equal to k_G when the driven gate area is the smallest, and equal to 1 in the other case.

The switching operation of MOS transistors is associated with losses of different natures that we take into account in the converter modeling: conduction (P_{cond}), switching (P_{SW}) and control gate (P_G). They are expressed as follows:

$$
\begin{aligned}
P_{cond} &= k_M r_{dson} I_{IN}^2 \\
&= k_M \left(\delta r_{nmos} + (1-\delta) r_{pmos} \right) I_{IN}^2 \\
P_{SW} &= f V_{OUT} I_{IN} t_{SW} \qquad (7) \\
P_G &= f \left((Q_{gn} + Q_{gp}) / k_M \right) V_G \\
&= 2f \left(Q_G / k_M \right) V_{OUT}
\end{aligned}
$$

Note that given the specific driver of MOS transistors, switching losses do not depend on the gate area. In addition to losses related to MOS transistors, we also take into account the copper losses of the inductance modeled by the series resistance r_L. The values of the converter parameters are specified in Table 2, and Fig. 7 illustrates the electrical model of the DC-DC converter. As we can see in Table 2, we take into account the variation of the channel resistance r_{dson} with the voltage applied between the gate and the source, here the output voltage V_{OUT}, but we assume the gate charge Q_G independent of the voltage.

Table 2: Values of the converter parameters

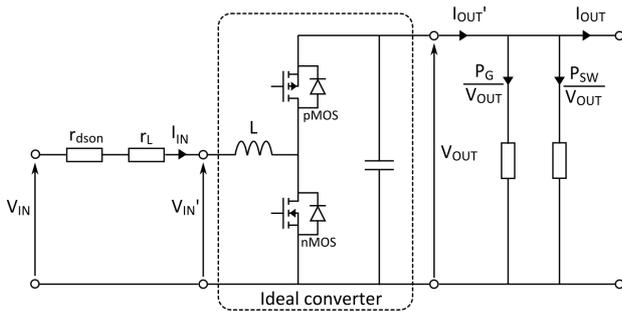| Parameters	Values
f	2.2×10^6 Hz
t_{SW}	70×10^{-9} s
Q_G	2×10^{-10} C
r_L	0.6 Ω
r_{nmos}	0.4 Ω for $V_{OUT}=3.3$V 0.3 Ω for $V_{OUT}=5$V
r_{pmos}	0.6 Ω for $V_{OUT}=3.3$V 0.4 Ω for $V_{OUT}=5$V

Figure 7: Electrical model of the DC-DC converter

For the LTC3537, we identified a factor k_G equal to 10. Fig. 8 shows the simulated efficiency curves with the parameters defined in Table 2 associated with experimental measurements, for an output voltage $V_{OUT}=3.3$V (which does not vary a lot here) and for different values of input voltage V_{IN} fundamentally variable in this application.
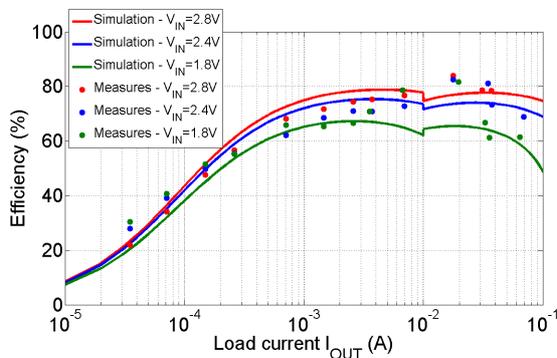

Figure 8: Simulated and measured efficiency curves of the LTC3537 for $V_{OUT} = 3.3$ V

In Fig. 8, we can easily observe the effect of switching gate area for a load current of 10 mA,

which is characterized by a discontinuity on the efficiency curve.

3.2. Electrical impedance matching corrected

At these power levels, major losses in the converter are switching losses which decrease when the input voltage increases. The best solution to reduce these losses is to integrate a maximum of thermocouples in the TEG. The TEG produced by Micropelt and Thermolife company are made of thin film. This technology makes it possible to integrate a greater density of thermocouples (about 5000 per cm^2 compared to 15 per cm^2 for the module TM-450-0.8-3.0 produced by Ferrotec company), and therefore to have high open circuit voltages E_G of TEGs relative to the area of the hot/cold plate. The solution discussed above to stack modules is also a way to increase E_G when the leg length is limited technologically.

Experimentally, we tested the boost converter LTC3537 from Linear Technology, connected to the TEG TM-450-0.8-3.0, and at its output to a Lithium-ion accumulator with a voltage $V_{OUT} = 4$V. By changing the regulatory structure of LTC3537, we were able to control it by regulating its input voltage V_{IN} to perform MPPT (maximum power point tracking) control [4]. We were then able to measure the input power P_{IN} (so the output power of the TEG) and the output power P_{OUT}. The results are described in Fig. 9. Moreover, thanks to models presented in the previous paragraph, we simulated this system of energy conversion and obtained the curves in solid lines in Fig. 9.
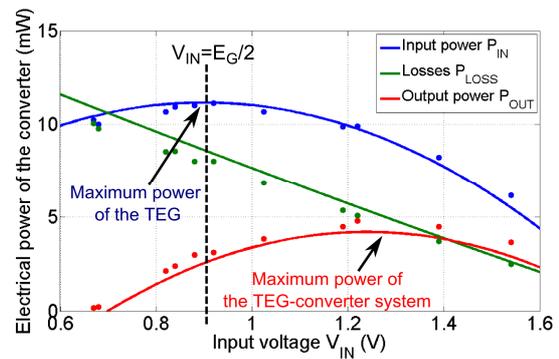

Figure 9: Experimental and simulated results of the LTC3537 converter

Thus, it appears that it might be interesting to sub-optimize the electrical matching by increasing the voltage V_{IN} (as compared to $E_G/2$, which correspond to the theoretical optimum) if we considered the converter losses.

4. System sizing optimization

In order to size a TEG to maximize electrical power produced while minimizing its volume, we introduced a bi-objective multi-variable optimization

algorithm based on particle swarm optimization [10] and Pareto dominance. This algorithm, called MOPSO, has been implemented in a Matlab environment in our laboratory and has already been used for another application [11]. We thus optimized the sizing of the TEG (with or without heat sink) for two different configurations. The first one consist in sizing the TEG connected to an ideal converter, i.e. we consider an electrical impedance matching (the TEG voltage is then equal to half its emf), and a converter efficiency of 100%. The second consist in optimizing the TEG connected to a DC-DC converter itself connected to a voltage source V_{OUT}=4V. In the following, we called it the TEG-converter system. In this configuration, we defined an optimization constraint requiring the TEG to generate sufficient voltage corresponding to the minimum operating voltage of the converter, i.e. 0.7V for the LTC3537. Therefore, given a number of optimization parameters (here S_{th}, l_{th} and h_d if presence of a heat sink), the optimization algorithm returned, after several iterations, a set of optimal solutions that meet the specifications requested and distributed on a Pareto front. The two competing criteria chosen are the minimization of the volume of the TEG and the heat sink (if it is present) and the maximization of the electrical power harvested. In addition, we forced the geometrical parameters to vary only in a bounded interval (see Table 3). For these optimizations, the temperature values of the body (T_b) and the ambient air (T_a) are those defined in Table 1. Finally, remember that we chose to vary the leg length, which amounts approximately to stack modules (except for the thickness of the alumina plates of the module).

Table 3: Bounded interval of the optimization geometrical parameters

Parameters	Min	Max
S_{th}	0	100cm^2
l_{th}	0	10cm
h_d	0	10cm

Figure 10 shows the solutions of the optimizations described above distributed on Pareto fronts.
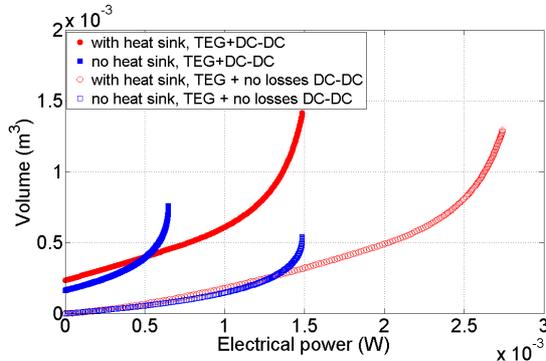

Figure 10: Bi-objective optimization solutions

We note that logically the electrical power produced by the TEG connected to an ideal converter is, given the volume of TEG, higher than that produced by the TEG-converter system. Indeed,

the additional conversion stage generates losses. Beyond this initial observation, we can notice that, from a certain volume, adding a heat sink makes it possible to harvest more power.

In Fig.11, the power density (power per unit volume) and the surface power density (power per unit area) have been plotted.
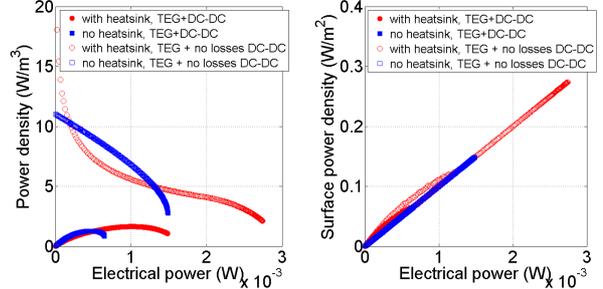

Figure 11: Evolution of the power density and the surface power density according to the electrical power

The better to interpret these results, we studied the evolutions of the optimization parameters, ie the surface area S_{th} (Fig. 12 and 13), the leg length l_{th} and the heat sink height h_d (Fig. 14 and 15), and also the evolutions of thermal resistances of the generator R_{thG} and the environment R_{thE} (Fig. 16 and 17).

For the sizing optimization of the TEG with an ideal DC-DC converter and harvesting the maximum power due to the electrical impedance matching (Fig. 12,14 and 16), we can observe that, without the heat sink presence, the surface area S_{th} chosen by the optimization algorithm is always the maximum allowed, i.e. here 100cm^2 (in blue in Fig. 12). Indeed, according to the equations (4) and (5), regardless of the electrical operating point of the TEG, its power is proportional to S_{th}. Thus, given a surface area, to increase the harvested power, we just have to increase the leg length l_{th} up to its optimum value (equation (6)). In Fig.14, the evolution of l_{th} finally corresponds to the increasing part of the graph P_{em} vs. l_{th}, shown in blue in Fig. 6. Once the maximum power is reached, the increase of l_{th} is no more profitable. In Figure 16, the evolution of the thermal resistances of the generator R_{thG} and the environment R_{thE} makes it obvious that the maximum power is achieved for a good thermal impedance matching, i.e. when $R_{thG}=R_{thE}$. This result is also observed when adding a heat sink. Moreover, with a heat sink, the reached powers are higher, the power increasing with the heat sink height h_d (equations (4) and (5)). The maximum power reached by the algorithm is when the heat sink height is equal to the maximum value allowed, i.e. by 10cm (Fig. 14).

Thus, for a desired electrical power and given heat exchange conditions, it is preferable to perform large surface areas and thin TEGs. In the case where a heat sink is added, TEGs with a heat sink height higher than the leg length are to be preferred.
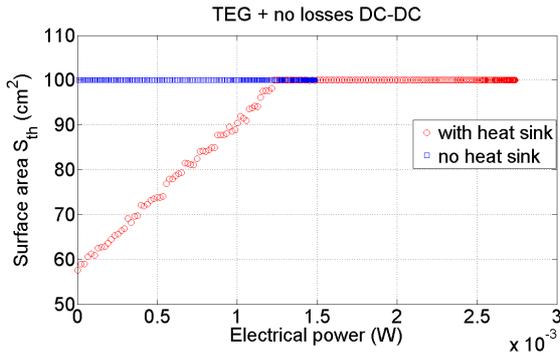
Figure 12 : Evolution of the surface area S_{th} according to the electrical power, for the TEG with an ideal converter
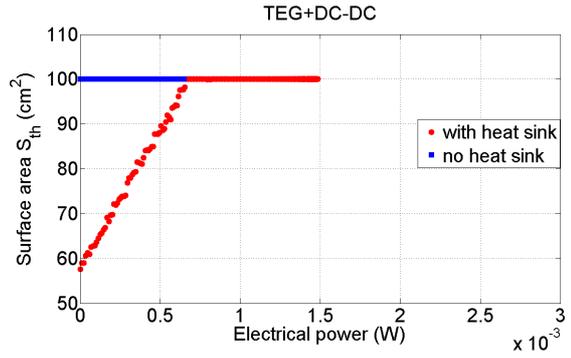

Figure 13 : Evolution of the surface area S_{th} according to the electrical power, for the TEG-converter system
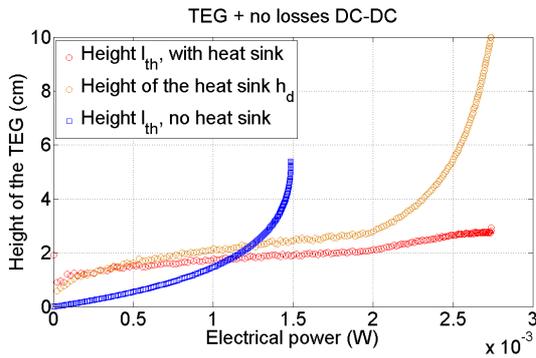

Figure 14 : Evolution of the heights, l_{th} and h_d, according to the electrical power, for the TEG with an ideal converter
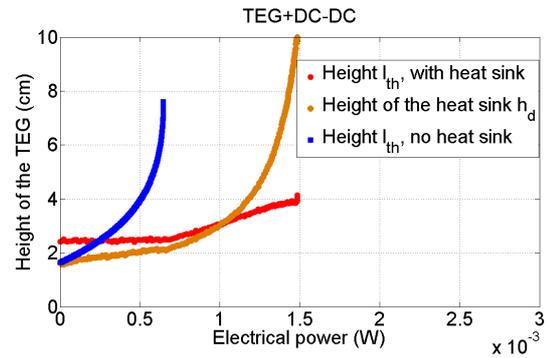

Figure 15 Evolution of the heights, l_{th} and h_d, according to the electrical power, for the TEG-converter system
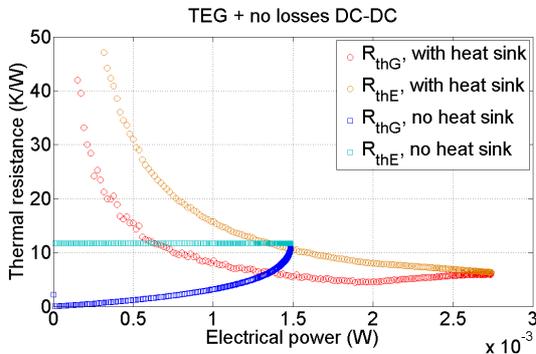

Figure 16 : Evolution of the thermal resistances, R_{thG} and R_{thE}, according to the electrical power, for the TEG with an ideal converter
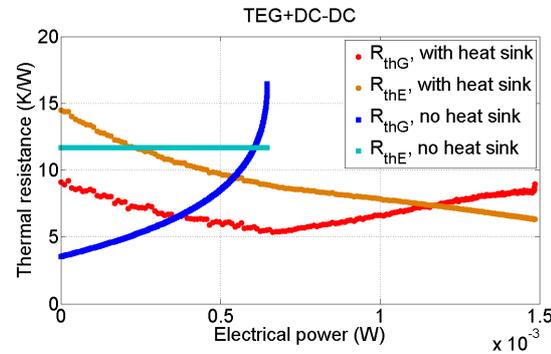

Figure 17 : Evolution of the thermal resistances, R_{thG} and R_{thE}, according to the electrical power, for the TEG-converter system

For the sizing optimization of the TEG-converter system (Fig. 13, 15 and 17), the results observed previously are no more available. Indeed, there is no more a thermal impedance matching when the harvested power is maximum. In addition, in observing the emf E_G of the TEG and input voltage of the converter V_{IN} (Fig. 18), we can note that the voltage V_{IN} is not equal to $E_G/2$ so there is not either an electrical impedance matching. Indeed, the voltage V_{IN} is always higher than $E_G/2$ so as to be sufficiently high to reduce converter losses and therefore maximize the output power of the TEG-converter system.
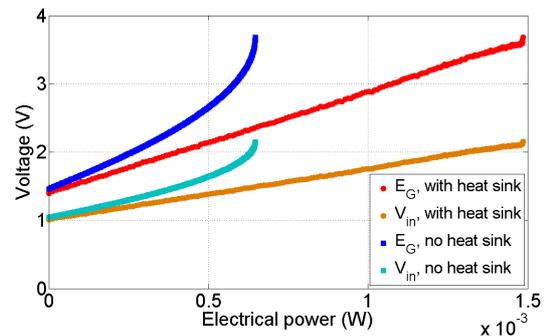

Figure 18: Evolution of the voltages E_G and V_{IN}, according to the electrical power, for the TEG-converter system

However, it is likely that the sizing of the converter is not well suited to this application. In Fig. 19, the converter efficiency for each solutions of the Pareto front was calculated, with the presence or not of a heat sink. The conversion efficiency reaches values around 40% without a heat sink, and 60% with a heat sink, but is very poor in low power. This observation highlights the interest to resize the converter, i.e. to integrate the converter sizing parameters to the global optimization, in order to obtain suitable converters that have higher conversion efficiencies in low power.
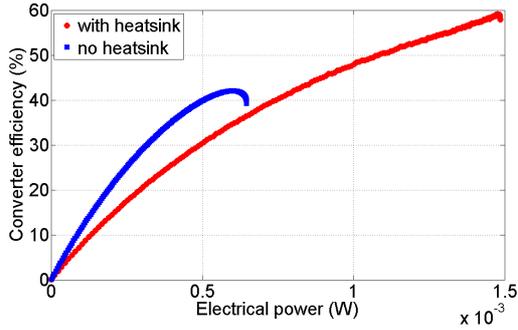

Figure 19: Converter efficiency according to the electrical power

To illustrate the thermal and electrical coupling of the whole system, Fig. 20 presents the power curves at the input (P_{IN}) and the output (P_{OUT}) of the converter, according to the legs length l_{th} for two different scenarios: maximizing the output power of the TEG (in blue) and maximizing the output power of the converter (in red). These curves have been plotted with the parameters defined in Table 1 and 2, except for the surface area S_{th} (and then the number of thermocouples N_{th}) which is here equal to 100 cm^2.
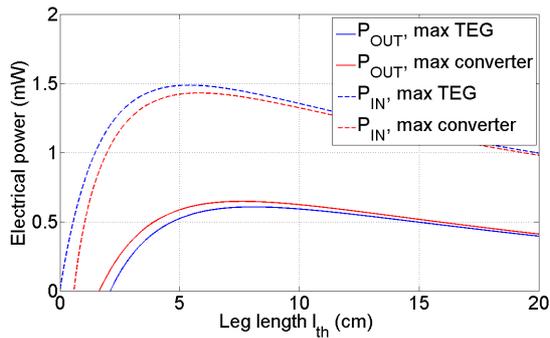

Figure 20: Input and output powers of the converter according to the leg length

In Fig. 20, we can first notice the sub-optimization of the theoretical electrical matching by noting that the output power P_{OUT} of the converter is slightly higher when maximizing the output power of the TEG-converter system (in red) rather than the output power of the TEG (in blue).

In addition, we also notice a thermal impedance mismatch. The leg length maximizing the output power of the TEG-converter system (here $l_{th\_opt} \approx 8cm$) is not the same as maximizing the

output power of the TEG (here $l_{th\_opt} \approx 5.5cm$). It is therefore more interesting to correct the thermal matching in taking into account all of the conversion chain. This latter observation explains the thermal resistances inequality observed in Fig. 17.

Finally, note that when one is interested in the TEG-converter system, there is a minimum leg length below which the power generated by the TEG is not sufficient to offset the converter losses which become excessive when the voltage is too low. In Fig. 15 and 20, the minimum leg length is approximately 2cm.

5. Conclusion

In this paper, we presented the study of a whole thermoelectric conversion chain incorporating the thermoelectric module(s), the DC-DC converter and a possible heat sink, in the project of thermal energy harvesting from the human body. Of course this approach can be extended to all applications, especially where low-power performance of DC-DC converter plays an important role. Thanks to the thermal and electrical models of the generator, the heat sink and the DC-DC converter, all based on experimental validation or on datasheets (heat sink), we were able, by introducing an optimization algorithm, to optimize the volume of TEG, with or without a heat sink and connected to an ideal or not DC-DC converter, in order to maximize its power harvested.

The study of TEG with an ideal converter highlights the relevance of the thermal matching of the TEG to its environment in order to maximize its power. This impedance matching can be done by increasing the leg length of the TEG, or when it is not technologically feasible, by stacking thermoelectric modules. However, when we take into account the losses of the DC-DC converter, we show, firstly, that it might be interesting to mismatch thermally the TEG impedance by not choosing the optimal leg length that maximizing its electrical power. Secondly, we highlight the interest of not working at the (theoritically) optimum electrical operating point by increasing the output voltage of the TEG (compared to $E_G/2$ corresponding to the maximum thermoelectric power) in order to reduce losses in the converter. Thus, this system approach enables us to optimize the whole system efficiency rather than the efficiency of each conversion stage of the electrical chain.

Nevertheless, the DC-DC converter studied is not necessarily well suited for all considered power level; we should therefore integrate the converter sizing parameters to the system optimization. Furthermore, the TEG studied has a low density of thermocouples. Technologies with higher density (although a priori theoretically less productive per unit area) could be better with such a system optimization thanks to the increasing of the converter efficiency.

References

[1] M. Lossec, B. Multon, H. Ben Ahmed, L. L'Hours, P. Quinton, J. Prioux et. al., "*Optimization Methodology for a Multi-Source-Energy Generation System using the Human Environment Energy Resource*", presented at NEST 2009, May 2008.

[2] D.M. Rowe, "*CRC Handbook of Thermoelectrics*", CRC Press, London, 1995.

[3] V. Leonov, T. Torfs, P. Fiorini, C. Van Hoof, "*Thermoelectric Converters of Human Warmth for Self-Powered Wireless Sensor Nodes*" IEEE Sensors Journal, 7, 650 (2007)

[4] M. Lossec, B. Multon, H. Ben Ahmed, C. Goupil, "*Thermoelectric generator placed on the human body: system modeling and energy conversion*", EPJAP, 52, 11103, Sept. 2010.

[5] E. Siivola, R.Mahadevan, P. Crocco, K. Von Gunten, D. Koester, "*Design considerations for TEG System Optimization*", Nextreme Thermal Solutions Inc. Whitepaper, 2010

[6] W. Glatz, S.Muntwyler, C.Hierold, "*Optimization and fabrication of thick flexible polymer based micro thermoelectric generator*", Sensors and Actuators A, 132, pp. 337-345, May 2006.

[7] V. Leonov, P.Fiorini , "*Thermal matching of a thermoelectric energy scavenger with the ambiance*", in Proc. Int. ECT07, Ukraine, pp.129–133.,2007

[8] LTC3537, Linear Technology, datasheet, 2.2 MHz, 600mA, Synchronous Step-Up DC/DC, Converter and 100mA LDO.

[9] R. Williams, W. Grabowski, A. Cowell, M. Darwish, and J. Berwick, "*The dual-gate W-switched power MOSFET: a new concept for improving light load efficiency in DC/DC converter*", in Proc. Int. ISPSD, 1997, pp. 193-196.

[10] M. Reyes-Sierra, C.A. Coello Coello, "*Multi-Objective Particle Swarm Optimizers: A Survey of the state-of-the-Art*", International Journal of Computational Intelligence Research, Vol. 2, No. 3, pp. 287-308, 2006

[11] J. Aubry, H. Ben Ahmed, B. Multon, "*Bi-Objective Sizing Optimization of a PM Machine Drive on an Operating Profile*", in Proc. Int. ICEM 2010, Rome